

# RSC Advances



This is an *Accepted Manuscript*, which has been through the Royal Society of Chemistry peer review process and has been accepted for publication.

*Accepted Manuscripts* are published online shortly after acceptance, before technical editing, formatting and proof reading. Using this free service, authors can make their results available to the community, in citable form, before we publish the edited article. This *Accepted Manuscript* will be replaced by the edited, formatted and paginated article as soon as this is available.

You can find more information about *Accepted Manuscripts* in the [Information for Authors](#).

Please note that technical editing may introduce minor changes to the text and/or graphics, which may alter content. The journal's standard [Terms & Conditions](#) and the [Ethical guidelines](#) still apply. In no event shall the Royal Society of Chemistry be held responsible for any errors or omissions in this *Accepted Manuscript* or any consequences arising from the use of any information it contains.

## ARTICLE

## Elastic models coupling the cellulose nanofibril to the macroscopic film level

Cite this: DOI: 10.1039/x0xx00000x

Gabriella Josefsson,<sup>a</sup> Gary Chinga-Carrasco<sup>b</sup> and E. Kristofer Gamstedt<sup>a</sup>

Received 00th January 2012,  
Accepted 00th January 2012

DOI: 10.1039/x0xx00000x

www.rsc.org/

The mechanical behaviour of cellulose nanofibrils is typically characterized by casting thin films and performing tensile tests on strips cut from these films. When comparing the stiffness of different films, the stiffness of the nanofibrils is only qualitatively and indirectly compared. This study provides some schemes based on various models of fibre networks, or laminated films, which can be used to assess the inherent stiffness of the nanofibrils from the stiffness of the films. Films of cellulose nanofibrils from different raw materials were manufactured and the elastic properties were measured. The expressions relating the nanofibril stiffness and the film stiffness were compared for the presented models. A model based on classical laminate theory showed the best balance between simplicity and adequacy of the underlying assumptions among the presented models. Using this model, the contributing nanofibril stiffness was found to range from 20 to 27 GPa. The nanofibril stiffness was also calculated from mechanical properties of nanofibril films found in the literature and compared with measurements from independent test methods of nanofibril stiffness. All stiffness values were found to be comparable and within the same order of magnitude.

### 1. Introduction

From a mechanical point of view, the cellulose microfibril constitutes the smallest structural building block of wood and is the main load-carrying constituent of wood. Wood pulp fibres can in principle be fibrillated into cellulose microfibrils, which correspond to the presently used term cellulose nanofibrils (CNFs).<sup>1,2</sup> CNF consists of crystalline and amorphous cellulose and has high stiffness and strength along the main axis compared with that of wood fibres. CNF is produced by a mechanical fibrillation process of pulp fibres, sometimes together with a pretreatment of the pulp to facilitate the separation of the nanofibrils. Mechanical fibrillation can be done through refining via a high pressure homogenizing process.<sup>3</sup> The refiner consists of a rotor and a stator disk where the pulp fibres are forced through a gap between these two parts. The fibres are thereby subjected to repeated stresses and the primary cell wall layer, P, and outer secondary cell wall layer, S1, are peeled off. A detrimental effect with the refining process is that the properties of the CNF can be impaired, e.g. reduction in degree of crystallinity and molar mass.<sup>4</sup> The use of pretreatment facilitates the fibrillation and makes the mechanical treatment more efficient.<sup>5,6</sup> It also seems to result in a more homogenous fibrillation of the fibres and generates elementary fibrils with a diameter of around 3-4 nm.<sup>7</sup>

<sup>a</sup> Uppsala University, Ångström Laboratory, Department of Engineering Sciences, Division of Applied Mechanics, Box 534, SE-751 21 Uppsala, Sweden

<sup>b</sup> Paper and Fiber Research Institute (PFI AS), Høgskoleringen 6b, NO-7491 Trondheim, Norway

The most practical way to characterize the mechanical properties of CNFs is tensile testing of strips cut from CNF films. The effect of wood species, chemical pretreatment and fibrillation process can then be compared. To relate the inherent CNF stiffness to that of the film, a suitable model must be used. The model should necessarily account for the structure of the material, i.e., among other factors, the nanofibril orientation distribution and the density of the material. Casting of CNF films typically means that the nanofibrils are deposited on a fine wire or a Petri dish, and the excess water is evaporated. If the suspension is well mixed and there is no flow, it can be assumed that the nanofibrils are deposited with a two-dimensional in-plane random orientation distribution. X-ray diffraction can be used to confirm that the out-of-plane orientation of fibrils is negligible.<sup>8</sup> The CNF film can then be regarded as a two-dimensional network of nanofibrils or a laminate depending on the density of the material. Most network models emanate from paper mechanics, where the assembly of the larger pulp fibres form a similar microstructure in paper sheets as what is expected of nanofibrils forming a CNF film. One of the first theories for modelling fibre networks was developed by Cox<sup>9</sup>. The model has been used to relate the

paper stiffness with the fibre stiffness but is also used for CNF films.<sup>10-12</sup> In the model by Cox, the fibres are assumed to be infinitely long and subjected to the same strain in their axial direction as that of the sheet in the same direction. Effects of fibre bending and fibre-fibre bonding are neglected. Page et al.<sup>13-15</sup> have suggested several modified models based on Cox' theory where finite fibre length and relative bonded areas in the sheet have been taken into account. Other models based on Cox' theory include influences from additional fibre features such as fibre curl, internal stresses, shear stress etc. One of those models was derived by van den Akker<sup>16</sup> where he assumes that even unbonded fibres can carry bending moments and shear stresses. Many of the more general models, however, include empirical parameters which cannot directly be determined independently. Krenchel<sup>17</sup> developed a model for fibre reinforced composite materials by defining an efficiency factor that depends on the orientation of the reinforcement fibres. The model can also be used for fibre networks and has been used by many authors to connect the elastic properties between CNFs and films.<sup>12,18-20</sup> Another widely used model for calculation of composite, or network<sup>21</sup>, stiffness is classical laminate theory (CLT), e.g. Tsai<sup>22</sup>. In CLT, the reduced stiffness matrix for an in-plane stress state of unidirectional plies is used to calculate the effective stiffness of a composite or a network. The composite or network is regarded as a laminate composed of these unidirectional plies with various orientations. The effective stiffness of the laminate is derived by averaging the plane-stress stiffness of the unidirectional plies.<sup>22</sup> The stiffness matrix of a ply with an off-axis orientation can be calculated through coordinate transformation. For quasi-isotropic composites, CLT has been further simplified by Tsai and Pagano<sup>23</sup>. The model is derived using several simplifications, where the final expression gives a simple relation between the composite stiffness and the in-plane Young's moduli of the unidirectional plies in the longitudinal and transverse directions, respectively.

To investigate the elastic properties of the nanofibrils, CNF films were produced from the pulp of *Radiata* pine and *Eucalyptus*, of which the former was also pretreated by TEMPO-mediated oxidation to facilitate the fibrillation. By measuring the tensile properties of the films, the elastic properties of the CNF can be calculated using a suitable micromechanical model. In this paper, the most commonly used micromechanical models connecting the film stiffness with the CNF stiffness are presented. Key differences in the assumptions of these models and their applicability to CNF films are discussed, such as the influence of the transverse elastic properties of the CNF to that of CNF film. The term 'micromechanical' should here be understood in a broader sense as a material model based on heterogeneous structure of the material, which may or may not be in the micrometre range. The stiffness of the CNFs is calculated from the stiffness of the produced films and compared with stiffness values found in the literature.

## 2. Modelling

Four common models have been investigated, namely (i) classical laminate theory (e.g. Tsai<sup>22</sup>), (ii) the Tsai-Pagano model<sup>22</sup>, (iii) the Cox model<sup>9</sup> and (iv) the Krenchel model<sup>17</sup>. They all have the advantage of being relatively simple, i.e. convenient analytical expressions without too many parameters which need to be experimentally quantified or estimated. Given the experimental scatter in stiffness measurements and input parameters, it is not motivated to use more complex and accurate numerical models for the purpose of screening the CNF stiffness. Finite element modelling can, however, be very useful for benchmarking different analytical models and to investigate effects of intrinsic features such as overlapping nanofibrils.<sup>24</sup> A too simple analytical model, which does not capture the main deformation mechanisms, would also not be a suitable choice. This balance between accuracy and simplicity is addressed with regard to the mentioned elastic models. The models have been developed for fibre network or composite materials with random orientated fibres, but could also be used for CNF films. The different models will give different values of the contributing stiffness of the CNFs, which can be compared with the stiffness estimated by other methods. In order to assess the reasons for these differences between the models, it is useful to understand the difference in assumptions in the various models. The predictive capability of various models can then be compared in relation to the underlying assumptions. The aim is to identify which assumptions are over-simplifying, and which are necessary to capture the mechanics of elastic deformation of nanofibril films. Abridged derivations of the various models, based on the original references, are therefore presented in the following, with the simplifying assumptions highlighted.

### 2.1 Classical laminate theory

Classical laminate theory (CLT) predicts the in-plane stiffness of a composite laminate composed of anisotropic two-dimensional layers or plies. CLT analogies are also used to describe the in-plane elasticity of non-layered materials, such as short-fibre composites<sup>25</sup>, paper sheets<sup>21</sup>, liquid crystals<sup>26</sup> and nanocomposites.<sup>27</sup> Each ply represents one specific orientation of the fibres and the off-axis stiffness matrix can be calculated through coordinate transformation. The relative thickness of the ply is related to the probability of the fibres within the specific orientation interval. The effective stiffness of the composite material or network is derived from the average plane-stress stiffness of unidirectional plies with various orientations. The plies can deform elastically in the longitudinal, transverse and shear directions in the plane. For a dense film of fibres with a random in-plane orientation distribution, the probability for each fibre direction is equal and the effective Young's modulus  $E^c$  becomes (e.g. Tsai<sup>22</sup>)

$$E^c = \frac{U_1^{p^2} - U_4^p}{U_1^p}, \quad (1)$$

where  $U_1^p$  and  $U_4^p$  are invariants of the reduced stiffness matrix of the hypothetical unidirectional plies from which the laminate is being constructed. The invariants can be expressed by

$$U_1^p = \frac{3}{8}Q_{11}^p + \frac{3}{8}Q_{22}^p + \frac{1}{4}Q_{12}^p + \frac{1}{2}Q_{66}^p, \quad (2)$$

and

$$U_4^p = \frac{1}{8}Q_{11}^p + \frac{1}{8}Q_{22}^p + \frac{3}{4}Q_{12}^p - \frac{1}{2}Q_{66}^p. \quad (3)$$

Here  $Q_{ij}^p$  are the reduced stiffness matrix elements of the unidirectional plies, which can be expressed as

$$Q_{11}^p = \frac{E_1^p}{1 - \nu_{12}^p \nu_{21}^p}, \quad (4)$$

$$Q_{12}^p = \frac{\nu_{21}^p E_1^p}{1 - \nu_{12}^p \nu_{21}^p}, \quad (5)$$

$$Q_{21}^p = Q_{12}^p, \quad (6)$$

$$Q_{22}^p = \frac{E_2^p}{1 - \nu_{12}^p \nu_{21}^p}, \quad (7)$$

and

$$Q_{33}^p = G_{12}^p, \quad (8)$$

where  $E_1^p$  is the longitudinal Young's modulus of the plies,  $E_2^p$  is the transverse Young's modulus,  $\nu_{12}^p$  and  $\nu_{21}^p$  are the in-plane Poisson ratios and  $G_{12}^p$  is the shear modulus.

For films of fibres, without a surrounding matrix, Eq. (4-8) will be functions of the fibre properties alone and the ply properties will be replaced by the fibre properties. The porosity of the film needs to be taken into account which could be done by scaling the isotropic Young's modulus, given in Eq. (1), with the ratio of the density of the porous film, and the density of the fibres. The effective Young's modulus becomes

$$E^{\text{film}} = \frac{\rho^{\text{film}}}{\rho^f} \frac{U_1^{f^2} - U_4^f}{U_1^f}. \quad (9)$$

## 2.2 The Tsai-Pagano model

The model developed by Tsai and Pagano<sup>23</sup> is used for estimation of the stiffness of composites or films with a quasi-isotropic lay-up and in-plane randomly oriented fibres.<sup>28-30</sup> The

model expresses the in-plane Young's modulus of layered composites in terms of the longitudinal and transverse Young's moduli of the constitutive unidirectional plies. However, the expression has been derived from CLT by making several simplifying assumptions. These assumptions will be outlined in the following in order to interpret the differences between the various models in predicting CNF stiffness from CNF film stiffness. The first simplification in the model is done by assuming that the Young's modulus of the random orientated composite material is equal to the invariant  $U_1$ , neglecting the fourth invariant  $U_4$  in Eq. (1). This assumption means that the Poisson ratio for the in-plane isotropic composite is considered as zero and that no deformation takes place in other direction than the direction of the far-field applied load. That approximation leads to the expression

$$E^c = \frac{3}{8}Q_{11}^p + \frac{3}{8}Q_{22}^p + \frac{1}{4}Q_{12}^p + \frac{1}{2}Q_{66}^p. \quad (10)$$

The idea with the model is then to express all components  $Q_{ij}^p$  in the reduced stiffness matrix as a function of the longitudinal and transverse Young's moduli of the unidirectional plies. For the components  $Q_{11}^p$  and  $Q_{22}^p$ , the same approximation is done as in Eq. (10), i.e. all deformations in other directions than an applied load are neglected, and the components  $Q_{11}^p$  and  $Q_{22}^p$  are approximated by

$$Q_{11}^p \cong E_1^p \quad (11)$$

and

$$Q_{22}^p \cong E_2^p. \quad (12)$$

This approximation is however more justified for the plies with a high degree of anisotropy, i.e. the 1 direction (fibre direction) is substantially stiffer than the 2 direction (transverse direction), where one of the Poisson ratios is close to zero. To obtain an expression for  $Q_{66}^p$ , Tsai and Pagano<sup>23</sup> used the elasticity solutions of longitudinal shear and transverse loading of a unidirectional composite ply developed by Adams and Doner,<sup>31,32</sup> given by

$$\frac{Q_{66}^p}{G^m} = \frac{G_{12}^p}{G^m} = F_1 \left( \frac{G^f}{G^m}, \nu^f \right) \quad (13)$$

and

$$\frac{Q_{22}^p}{E^m} = \frac{E_2^p}{E^m} = F_2 \left( \frac{E^f}{E^m}, \nu^f \right). \quad (14)$$

It is also assumed that the function  $F_1$  and  $F_2$  are related to each other as

$$F_1 = \beta F_2, \quad (15)$$

where  $\beta$  is a function of the fibre volume fraction and the constituents stiffness ratio. By using the well-known elastic relation for the isotropic matrix

$$G^m = \frac{E^m}{2(1 + \nu^m)}, \quad (16)$$

together with equations (13-15), a relation between  $Q_{66}^p$  and  $E_2^p$  can be made as

$$Q_{66}^p = \frac{\beta E_2^p}{2(1 + \nu^m)}. \quad (17)$$

For most polymer matrix materials the Poisson ratio  $\nu^m$  is around 0.3<sup>33</sup> and by using a Poisson ratio of 1/3, Eq. (17) can be simplified and written

$$Q_{66}^p = \frac{3}{8} \beta E_2^p. \quad (18)$$

The off-axis component  $Q_{12}^p$  can be expressed by the transverse Young's modulus and the Poisson ratio  $\nu_{12}^p$  of the unidirectional composite plies by

$$Q_{12}^p = \nu_{12}^p E_2^p, \quad (19)$$

where this approximation is based on the assumption that the smaller Poisson ratio  $\nu_{21}^p$  is close to zero.

By the steps described above, all reduced components  $Q_{ij}^p$  are now described as functions of the longitudinal Young's modulus and the transverse Young's modulus of the composite plies. These expressions can now be inserted in Eq. (10), which describes the average Young's modulus of a composite of random orientated fibres as

$$E^c = \frac{3}{8} E_1^p + \frac{3}{8} E_2^p + \frac{1}{4} \nu_{12}^p E_2^p + \frac{1}{2} \beta E_2^p. \quad (20)$$

By using a Poisson ratio  $\nu_{12}^p$  of 1/4 and a  $\beta$  of 1, Eq. (20) can be written as<sup>23</sup>

$$E^c = \frac{3}{8} E_1^p + \frac{5}{8} E_2^p. \quad (21)$$

The Young's modulus of a film, or network, will be a function of the two fibre moduli alone, and can be scaled in the same way as the CLT model in Eq. (9) to account for the porosity of the film. The Young's modulus of a film, or network of fibres, will then be given by

$$E^{\text{film}} = \frac{\rho^{\text{film}}}{\rho^f} \left( \frac{3}{8} E_1^f + \frac{5}{8} E_2^f \right). \quad (22)$$

### 2.3 The Cox model

The model by Cox<sup>9</sup> is derived directly for a network of fibres or a fibrous material where the fibres are assumed to be infinitely long and extend from one side of the sample to the other. It is also assumed that the fibres are not connected, and can carry loads only in the fibre ends. Furthermore, the flexural stiffness of the fibres is neglected so that the fibres can carry load only in tension. If the sheet is subjected to axial strains in two directions,  $\varepsilon_x^{\text{film}}$  and  $\varepsilon_y^{\text{film}}$ , and a shear strain  $\gamma^{\text{film}}$ , the axial strain in a fibre that lies at a certain angle  $\varphi$  from the  $x$ -axis, would be  $\varepsilon_1^f = \varepsilon_x^{\text{film}} \cos^2 \varphi + \varepsilon_y^{\text{film}} \sin^2 \varphi + \gamma^{\text{film}} \cos \varphi \sin \varphi$ . The load in the fibre is proportional to the axial strain and the contribution of the fibre to the loads in the  $x$  and  $y$  direction is the product with  $\cos \varphi$  and  $\sin \varphi$ , respectively. The probability of a fibre having the specific orientation  $\varphi$  from the  $x$ -axis is given by the distribution function  $f(\varphi)$ . For that specific orientation, the number of fibres which intersect a line of a unit length perpendicular to the  $x$ -axis is  $f(\varphi) \cos \varphi$ , and the number of fibres which intersect a line of a unit length perpendicular to the  $y$ -axis is  $f(\varphi) \sin \varphi$ . The loads per unit width can then be defined as

$$P_x^{\text{film}} = K_1^f \int_0^\pi (\varepsilon_x^{\text{film}} \cos^2 \varphi + \varepsilon_y^{\text{film}} \sin^2 \varphi + \gamma^{\text{film}} \cos \varphi \sin \varphi) \cos^2 \varphi f(\varphi) d\varphi, \quad (23)$$

$$P_y^{\text{film}} = K_1^f \int_0^\pi (\varepsilon_x^{\text{film}} \cos^2 \varphi + \varepsilon_y^{\text{film}} \sin^2 \varphi + \gamma^{\text{film}} \cos \varphi \sin \varphi) \sin^2 \varphi f(\varphi) d\varphi, \quad (24)$$

and

$$T^{\text{film}} = K_1^f \int_0^\pi (\varepsilon_x^{\text{film}} \cos^2 \varphi + \varepsilon_y^{\text{film}} \sin^2 \varphi + \gamma^{\text{film}} \cos \varphi \sin \varphi) \cos \varphi \sin \varphi f(\varphi) d\varphi, \quad (25)$$

where  $K_1^f$  is the product of the fibre Young's modulus and the ratio of the density of the film and the density of a fibre.

After determining the integrals, the forces can be rewritten as

$$P_x^{\text{film}} = C_{11}^f \varepsilon_x^{\text{film}} + C_{12}^f \varepsilon_y^{\text{film}} + C_{16}^f \gamma^{\text{film}}, \quad (26)$$

$$P_y^{\text{film}} = C_{12}^f \varepsilon_x^{\text{film}} + C_{22}^f \varepsilon_y^{\text{film}} + C_{26}^f \gamma^{\text{film}}, \quad (27)$$

and

$$T^{\text{film}} = C_{16}^f \varepsilon_x^{\text{film}} + C_{26}^f \varepsilon_y^{\text{film}} + C_{66}^f \gamma^{\text{film}}. \quad (28)$$

The orientation distribution function must be periodic and can thereby be written as the sum

$$f(\varphi) = \frac{1}{\pi} (1 + a_1 \cos 2\varphi + a_2 \cos 4\varphi + a_3 \cos 6\varphi + \dots + b_1 \sin 2\varphi + b_2 \sin 4\varphi + b_3 \sin 6\varphi + \dots) \quad (29)$$

Terms of higher order than 2 will not affect the elastic constants. The stiffness parameters can then be expressed as

$$C_{11}^f = \frac{K_1^f}{16}(6 + 4a_1 + a_2), \quad (30)$$

$$C_{22}^f = \frac{K_1^f}{16}(6 - 4a_1 + a_2), \quad (31)$$

$$C_{12}^f = C_{66}^f = \frac{K_1^f}{16}(2 - a_2), \quad (32)$$

$$C_{16}^f = \frac{K_1^f}{16}(2b_1 + 4b_2), \quad (33)$$

and

$$C_{26}^f = \frac{K_1^f}{16}(2b_1 - 4b_2). \quad (34)$$

For a random in-plane orientation, all constants  $a_1$ ,  $a_2$ ,  $b_1$ ,  $a_2$ , are zero, and the Young's modulus of the fibre sheet becomes

$$E^{\text{film}} = K_1^f/3, \quad (35)$$

or

$$E^{\text{film}} = \frac{1}{3} \frac{\rho^{\text{film}}}{\rho^f} E_1^f. \quad (36)$$

#### 2.4 The Krenchel model

Krenchel<sup>17</sup> assumed, as Cox, that the fibres cannot carry load in the transverse direction and that the flexural stiffness is negligible. He derived an efficiency factor of reinforcement, which is determined by summation of the reinforcement of pairs of parallel fibres in an angle-ply lay-up. In the derivation by Krenchel, it is assumed that a rectangular plane of a composite material consists of a balanced symmetric configuration of layers with the same amount of fibres with an orientation of  $\pm \varphi$  from the  $x$ -axis. The composite is subjected to an external force in the  $x$ -direction. The Poisson ratio is assumed to be zero for both the fibres and the matrix, such that no deformation takes place in other directions than the direction of an applied load. A fibre oriented at an angle  $\varphi$  from the  $x$ -axis, extending from one side of a rectangular composite plate to the opposite one, is assumed to initially have unit length. The composite has then an initial length of  $\cos\varphi$ . For an elongation  $\varepsilon_1^f$  of the unit length fibre along the fibre direction, an applied force  $P_1^f$  is required. This force can be divided in two components,  $P_x^f = P_1^f \cos \varphi$  and  $P_y^f = P_1^f \sin \varphi$ , where the component in the  $y$ -direction will be cancelled by the corresponding component from a fibre with the orientation  $-\varphi$ . From the external force, the composite will be subjected to a strain,  $\varepsilon_x^c$ , and the elongation of the composite, with an original

length of  $\cos \varphi$ , will be  $\varepsilon_x^c \cos \varphi$ . Thereby, the elongation of the fibre can be written as a function of the elongation of the composite as

$$\varepsilon_1^f = \varepsilon_x^c \cos^2 \varphi. \quad (37)$$

With Hooke's law, the fibre force can be written

$$P_1^f = E_1^f \varepsilon_1^f \Delta S_0^f = E_1^f \varepsilon_x^c \cos^2 \varphi \Delta S_0^f, \quad (38)$$

where  $\Delta S_0^f$  is the area of the fibre perpendicular to the fibre length which can be expressed by the fibre area perpendicular to the  $x$ -axis by

$$\Delta S_0^f = \Delta S_x^f \cos \varphi. \quad (39)$$

Eq. (38) can be rewritten as a function of the  $x$ -components of the force and the cross section area of the fibre by

$$P_x^f / \cos \varphi = E_1^f \varepsilon_x^c \cos^2 \varphi \Delta S_x^f \cos \varphi, \quad (40)$$

or

$$P_x^f = E_1^f \varepsilon_x^c \Delta S_x^f \cos^4 \varphi. \quad (41)$$

For a force in the  $x$ -direction, the effective area of a fibre is  $\Delta S_x^{f'} = \Delta S_x^f \cos^4 \varphi$ . By summation over all fibres in the cross section, the total effective area becomes

$$S_x^{f'} = \sum_n \Delta S_{x n}^{f'} = \sum_n \Delta S_{x n}^f \cos^4 \varphi_n. \quad (42)$$

With this expression of the effective area of the fibres, the efficiency factor of reinforcement of arbitrary orientation can be expressed by

$$\eta = \frac{S_x^{f'}}{S_x^f} = \frac{\sum_n \Delta S_{x n}^f \cos^4 \varphi_n}{S_x^f}, \quad (43)$$

where  $S_x^f$  is the total area of the fibres in a cross section perpendicular to the  $x$ -axis. It can be shown that the ratio between  $\Delta S_{x n}^f$  for a group of parallel fibres and  $S_x^f$  is the particular proportion,  $a_n$ , of that group with respect to total reinforcement, i.e. the probability of the fibres having the specific orientation  $\varphi_n$ . The efficiency factor can then be written

$$\eta = \sum_n a_n \cos^4 \varphi_n. \quad (44)$$

For a continuous distribution of the fibre orientation, the sum is replaced by integration. For the case of a random in-plane distribution, the efficiency factor becomes

$$\eta = \int_{-\pi/2}^{\pi/2} \frac{1}{\pi} \cos^4 \varphi d\varphi = \frac{3}{8}. \quad (45)$$

With the expression of the efficiency factor, the effective Young's modulus for a composite consisting of fibres with longitudinal Young's modulus,  $E_1^f$ , and a matrix with a Young's modulus,  $E^m$ , is then given by

$$E^c = \beta \eta E_1^f + (1 - \beta) E^m, \quad (46)$$

where  $\beta$  is the volume fraction of the inclusion. For a fibre network, i.e. without matrix, or the Young's modulus of the matrix can be considered zero,  $\beta$  can be regarded as a measurement of how dense the fibre network is relative to the amount of pores. In other words, for fibre network can  $\beta$  be described as the relation between the network density and the density of the fibres as

$$\beta = \frac{\rho^{\text{film}}}{\rho^f}. \quad (47)$$

Eq. (46) then becomes

$$E^{\text{film}} = \frac{\rho^{\text{film}}}{\rho^f} \eta E_1^f, \quad (48)$$

where  $\eta$  is 3/8 for a film with randomly oriented fibres.

### 3. Experimental procedures

#### 3.1 Materials

Three series of CNF suspensions were produced from hardwood *Eucalyptus* and softwood *Pinus radiata* kraft pulp fibres, as described by Syverud et al.<sup>34</sup>. Some of the softwood pulp was pretreated with TEMPO mediated oxidation according to Saito et al.<sup>5</sup>.

#### 3.2 Preparation of CNF films

The CNF suspensions were diluted to 0.1 wt% fibril consistency and stirred well. The suspensions were poured into funnels, with bottoms consisting of a filter paper on a fine copper grid, and subsequently dewatered. The diameter of the funnels was 60 mm. A total of 10 films, with the dry basis weight of 20 g/m<sup>2</sup>, were produced from each type of CNF. After dewatering, the films were placed in an oven, 100 °C for 1 hour, to completely remove the moisture.

#### 3.3 Tensile testing

The films were cut in stripes with 10 mm in width and 35-60 mm in length and placed in a climate room at 23 °C and 55% relative humidity for 24 hours of conditioning. The elastic properties were measured with Zwick material tester, model 2005. The gauge length for the strain measurements was 20 mm. Since only the elastic properties and not the strength was

characterised, rectangular strips were tested rather than dog-bone shaped specimens.

## 4. Results and discussion

CLT describes the elastic properties of a film, or a layered composite, from the anisotropic elastic properties of the constituent layers. It takes into account all in-plane elastic constants, and accounts for axial, transverse and shear stresses in a ply with a given orientation. In comparison to CLT, Cox, as well as Krenchel, assumes that the fibres can only carry load in tension, and all other load cases are neglected. The assumption that the film stiffness is a function of only the axial stiffness of the fibres would be the same as to assume that all other elastic moduli are equal to zero. The model by Tsai and Pagano is originally derived for composite materials but the final expression can be used for fibre films or CNF films. Although it takes into account all types of in-plane loading, a lot of approximations are done in the derivations. To graphically show the influence of the assumptions in the various models, the Young's modulus of a dense film of CNF, in the models regarded as a network of fibres, has been calculated as a function of the transverse Young's modulus  $E_2^f$  of the CNF. A plausible value of the axial Young's modulus  $E_1^f = 50$  GPa was chosen. In CLT, three different shear moduli were used,  $G_{12}^f = E_1^f/5$ ,  $G_{12}^f = E_1^f/10$  and  $G_{12}^f = 0$ . The longitudinal Poisson ratio,  $\nu_{12}^f$ , was chosen to 0.25 and the transverse Poisson ratio can be calculated with the other elastic constants by

$$\nu_{21}^f = \frac{E_2^f}{E_1^f} \nu_{12}^f. \quad (49)$$

The Young's modulus of a film, calculated with the different models, is shown in Fig. 1.

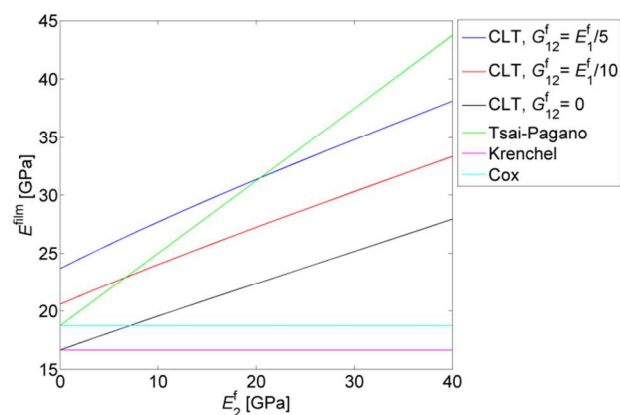


Fig. 1. Young's modulus of a CNF film, as a function of the transverse Young's modulus of the CNF, calculated with different models.

The plot in Fig. 1 shows that for small transverse Young's moduli and shear moduli of the CNF, the models give similar results. As the transverse modulus and shear modulus increase, the difference between the models increases. For a high

transverse and shear modulus, both the Cox model and the Krenchel model predict a stiffness that is less the half of the stiffness predicted by CLT. For dense films, where transverse and shear loading of the CFN is probable, CLT is preferable since it accounts for these loading modes separately. The Cox and Krenchel models, however, are more suitable for low-density unconsolidated paper materials, which can be regarded as a loose network, where only axial forces are considered in the reinforcing units. The Tsai-Pagano model falls somewhere between CLT and the network models as shear loading is indirect taken into account by the assumption that the shear modulus is related to the transverse Young's modulus. For a more accurate estimation of CNF stiffness or its contribution to film stiffness, finite element modelling could be used. Kulachenko et al.<sup>24</sup> found thorough numerical simulations that for thin CNF sheets, the relative stored elastic energy in bending is most considerable. They also found that strain field is not uniform under uniform and uniaxial loading. Bending arise in the fibrils that are draped over the underlying fibrils and from the non-uniform strain field due to the structural heterogeneity. The analytical models used in the present work do not include bending deformation in the nanofibrils and assume iso-strain conditions in the film, which limits their applicability to dense and thick CNF films. The basis weight of the present material is 20 g/m<sup>2</sup> and the thickness 14-21 μm. This would form a homogeneous material with up to three orders of magnitudes of CNF layers, based on a CNF or microfibril diameter of 20 nm.<sup>35</sup>

During the last decade, there has been a significant increase in research aiming to develop CNF materials. Many studies focus on the preparation of CNF films, which is usually technically more straightforward than to produce CNF-based foams<sup>36</sup> and bulk composites<sup>37</sup>. Published works on CNF films typically investigate the tensile behaviour of the film rather than addressing the mechanical properties of the nanofibrils themselves. By applying CLT, an estimation of the elastic properties of the CNF can however be obtained. Considering the most popular network models outlined above, CLT is most likely the model that best captures the mechanical behaviour of the films since it includes the in-plane anisotropic behaviour of the nanofibrils. In order to back-calculate the CNF stiffness with CLT, the stiffness and the porosity of the films have to be measured. For the films in this study, the film thicknesses have been documented by Chinga-Carrasco et al.<sup>35</sup> by scanning electron microscopy (SEM). By using a CNF density of 1.5 g/cm<sup>3</sup>, the porosity of the films was calculated from the thickness and the dry base weight. Measurements with a conventional micrometre screw gauge are known to overestimate the thickness, and quantification of film thickness is preferably done by SEM of polished cross-sections.<sup>35</sup> The thicknesses of the different films are presented in Table 1. The degree of polymerisation, chemical composition and a rough size distribution of the CNFs have been characterised by Syverud et al.<sup>34</sup>

**Table 1** Thickness values of the films measured with SEM<sup>35</sup>

Fibril raw material	Pretreatment	Thickness (μm)
<i>Eucalyptus</i>	None	20.65±1.17
<i>Pinus radiata</i>	None	18.20±1.18
<i>Pinus radiata</i> ,	TEMPO mediated oxidation	14.97±0.45

From the initial linear part of the stress-strain curve, the Young's modulus of the films was determined. CLT was used to back-calculate the effective Young's modulus of the fibrils. The orientation distribution of the CNFs was assumed to be random in the plane, since the nanofibrils were slowly deposited on the wire during dewatering without any stirring or flow.<sup>38</sup> The SEM image in Fig. 2 shows a film made of *Pinus Radiata* CNFs and does not indicate any preferential fibril orientation in the plane.

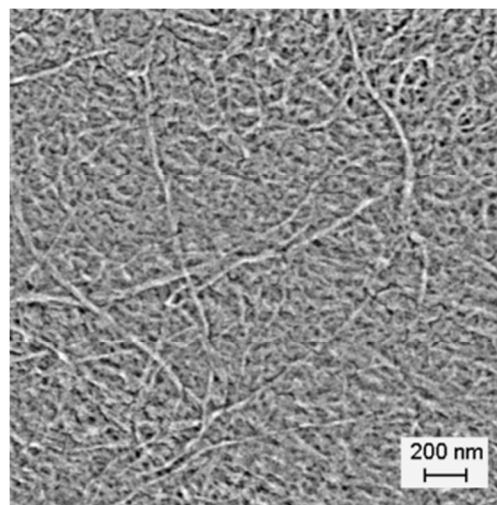


**Fig. 2** A SEM image of the in-plane random orientated fibrils in a film made from *Pinus Radiata*.

Table 2 summarizes the identified fibril stiffness values of the experimentally investigated films, as well as of various CNF films presented in literature. The ratios of the Young's moduli of the nanofibrils, used in the CLT, were based on self-consistent Mori-Tanaka calculations of nanofibril stiffness described by Josefsson et al.<sup>39</sup>. From the calculation described in paper, the stiffness matrix of the fibril becomes

$$C = \begin{pmatrix} 69 & 8.8 & 8.8 & 0 & 0 & 0 \\ 8.8 & 27 & 9.4 & 0 & 0 & 0 \\ 8.8 & 9.4 & 27 & 0 & 0 & 0 \\ 0 & 0 & 0 & 8.8 & 0 & 0 \\ 0 & 0 & 0 & 0 & 3.5 & 0 \\ 0 & 0 & 0 & 0 & 0 & 3.5 \end{pmatrix} [\text{GPa}].$$

Based on this stiffness matrix, the transverse Young's modulus of the fibrils was taken to be 1/3 of the longitudinal Young's modulus and the shear modulus was taken to be 1/20 of the longitudinal Young's modulus. The Poisson ratios were set to  $\nu_{LT} = 0.24$  and  $\nu_{TL} = 0.09$ , directly taken from the stiffness matrix. With these assumptions, the stiffness of the films will

be a function of only the axial Young's modulus of the fibrils and the film porosity in the CLT model in Eq. (9). For the present materials, it can be noticed in Table 2, that hardwood Eucalyptus CNFs are effectively stiffer than the ones from the softwood *Pinus radiata*. This is also consistent with the effective stiffness of pulp fibres determined from tensile tests of pulp composites, where the Eucalyptus fibres are stiffer than those from pine.<sup>25</sup> It can also be noted in Table 2 that TEMPO pretreatment of the softwood results in stiffer CNFs, which is expected since the treatment facilitate the fibrillation while

limiting mechanical damage of the nanofibrils<sup>40</sup>. The stiffness of the present CNFs, 20-27 GPa, were found to be lower than nanofibril stiffness values obtained from literature values of softwood pulp CNF films, ranging between 33 and 39 GPa, with an exceptional value of 61 GPa, as presented in Table 2. At this stage, we cannot explain why the present CNFs are less stiff than values obtained in other studies, but the table serve to show that quantitative stiffness comparisons of different types of CNFs can be made from macroscopic tensile testing of films.

**Table 2** Fibril stiffness back-calculated from film stiffness using the CLT model. The films are made of fibrils extracted from different kinds of wood pulp using different kinds of pretreatment and processing methods. In some papers, the porosity or the density are not given. These values have then been calculated from other given quantities, including the specific modulus and the assumption that CNF density is 1.5 g/cm<sup>3</sup>. The calculated values are given in italic.

Fibril type / pretreatment	Film Young's modulus [GPa]	Thickness [ $\mu\text{m}$ ]	Density [ $\text{g}/\text{cm}^3$ ]	Porosity [%]	Fibril Young's modulus [GPa]	Reference
Softwood / no pretreatment	9.7	18.2 $\pm$ 1.18	1.14	24	20	<i>This work</i>
Hardwood / no pretreatment	8.5	20.7 $\pm$ 1.17	1.06	29	25	<i>This work</i>
Softwood / TEMPO pretreatment	12.7	15.0 $\pm$ 0.45	1.56	0	27	<i>This work</i>
Softwood / enzymatic pretreatment	14	70	1.34	10.5	33	Henriksson and Berglund <sup>41</sup>
Softwood / no pretreatment	16	1500-2000	1.48	1.33	34	Yano and Nakahara <sup>42</sup>
Softwood / enzymatic pretreatment	14.7	60-80	1.22	19	38	Henriksson et al. <sup>43</sup>
Softwood / N/A	13.5	50	1.08	28	39	Sehaqui et al. <sup>44</sup>
Softwood / no pretreatment	15.7	21	0.81	45.9	61	Syverud and Stenius <sup>11</sup>

In principle, the stiffness of fibrils extracted from different raw materials, using different pretreatments and fibrillation processes could be investigated from films of various porosities, thicknesses and orientation distributions, provided that the underlying assumptions of the model are acceptable. This could potentially be a helpful characterization method to be used in development of load-carrying CNF materials.

To compare the effective fibril stiffness obtained by inverse modelling, CNF stiffness values measured by other independent methods are compiled in Table 3. The values obtained by the present method are consistently lower than those obtained by other methods, i.e. directly (bending in an atomic force microscope<sup>45</sup>), indirectly (back-calculation from composite stiffness<sup>46</sup>) or predicted (finite elements model and assumed elastic properties of the polymer constituents<sup>47</sup>). A contributing factor could be that the CNFs are considered to be infinitely long with perfect stress transfer in all directions in the plane. Also, the scatter could be affected by differences in moisture content. The ambient conditions affecting the moisture absorption was not uniform and sometimes not even documented in the cited studies. More work is needed to validate and compare different methods to estimate the fibril stiffness, preferably with the same type of material and same testing conditions. Those methods, such as the present, which rely on a simplified analytical model to identify the fibril stiffness, should be compared with more exact numerical models, where detailed features of the nanostructure and a full

description of the properties of the fibrils are considered<sup>24</sup>. Nevertheless, the present approach gives stiffness values in the

right order of magnitude and could probably be used to rank the stiffness of the constitutive fibrils in a wide variety of films.

**Table 3** Comparison of fibril stiffness estimated with different methods

Method	Fibril Young's modulus [GPa]	Reference
Back-calculation from films	20-61	<i>This work. See Table 2 for references</i>
AFM bending	61-107	Cheng et al. <sup>45</sup>
Finite element method	63-82	Persson <sup>47</sup>
Back-calculation from composite material	65	Josefsson et al. <sup>46</sup>

## 5. Conclusions

The contributing stiffness of the CNFs can be determined from the measured macroscopic in-plane stiffness of CNF films. A number of established analytical models were compared with respect to the relation between CNF and film stiffness. It was found that CLT was the only model among the tested ones to directly account for the effect of transverse and shear stiffness of the CNFs. The models by Cox and Krenchel only included the axial fibril stiffness. The Tsai-Pagano model includes the effect of transverse fibril stiffness, but assumes that the shear stiffness is proportional to transverse stiffness. For a dense CNF film, all in-plane loading modes are expected, and the analogy with CLT was chosen as the best option, in terms of simplicity and physicality.

The back-calculated Young's modulus of the CNFs extracted from hardwood and softwood pulp (with and without TEMPO oxidation pretreatment) ranged from 20 to 27 GPa. This is somewhat lower than values for other CNFs obtained from film stiffness values found in the literature. Pretreatment resulted in higher stiffness values, and hardwood CNFs were found to be stiffer than the softwood ones.

The presented back-calculation scheme can be used to estimate the Young's modulus of the CNFs making up the thin dense fibrillar films. In absolute terms, more work is required to validate the method, e.g. by comparison with independent test methods and more accurate numerical models. For ranking CNF stiffness for materials development purposes, the proposed method shows the advantage of a combination of experimental simplicity and straightforward calculations.

### Acknowledgement

The authors would like to acknowledge the support from the COST Action FP0802 (Experimental and Computational Micro-Characterization Techniques in Wood Mechanics) for short-time scientific mission to carry out carry out the experimental work.

### References

- 1 A. F. Turbak, F. W. Snyder, and K. R. Sandberg, *Journal of Applied Polymer Science* **37**, 815 (1983).
- 2 G. Chinga-Carrasco, *Nanoscale Research Letters* **6**, 1 (2011).
- 3 S. Iwamoto, A. N. Nakagaito, and H. Yano, *Applied Physics A* **89**, 461 (2007).
- 4 M. Henriksson, G. Henriksson, L. A. Berglund, and T. Lindström, *European Polymer Journal* **43**, 3434 (2007).
- 5 T. Saito, Y. Nishiyama, J.-L. Putaux, M. Vignon, and A. Isogai, *Biomacromolecules* **7**, 1687 (2006).
- 6 L. Wågberg, G. Decher, M. Norgren, T. Lindstrom, M. Ankerfors, and K. Axnas, *Langmuir* **24**, 784 (2008).
- 7 T. Saito, S. Kimura, Y. Nishiyama, and A. Isogai, *Biomacromolecules* **8**, 2485 (2007).
- 8 H. Nilsson, S. Galland, P. T. Larsson, E. K. Gamstedt, T. Nishino, L. A. Berglund, and T. Iversen, *Composites Science and Technology* **70**, 1704 (2010).
- 9 H. Cox, *Brit. J. Appl. Phys.* **3**, 72 (1952).
- 10 C. Aulin, M. Gällstedt, and T. Lindström, *Cellulose* **17**, 559 (2010).
- 11 K. Syverud and P. Stenius, *Cellulose* **16**, 75 (2009).
- 12 A. Retegi, N. Gabilondo, C. Pena, R. Zuluaga, C. Castro, P. Ganan, K. de La Caba, and I. Mondragon, *Cellulose* **17**, 661 (2010).
- 13 D. Page, R. Seth, and J. De Grace, in *Mechanics of Flexible Fibre Assemblies* (1980), p. 419.
- 14 D. Page and R. Seth, *Tappi* **63**, 113 (1980).
- 15 D. Page and R. Seth, *Tappi J* **63**, 99 (1980).
- 16 J. Van den Akker, *Some theoretical considerations on the mechanical properties of fibrous structures*, Vol. 1 (Technical Section B.P. and B.M.A., London, 1962).
- 17 H. Krenchel, *Fibre reinforcement* (Alademisk forlag, 1964).
- 18 R. Rusli and S. J. Eichhorn, *Applied Physics Letters* **93**, 033111 (2008).
- 19 S. J. Eichhorn and R. J. Young, *Cellulose* **8**, 197 (2001).
- 20 A. Šturcová, G. R. Davies, and S. J. Eichhorn, *Biomacromolecules* **6**, 1055 (2005).

- 21 L. A. Carlsson and C. N. Fellers, *Fibre Science and Technology* **13**, 213 (1980).
- 22 S. W. Tsai, *Theory of composites design* (Think composites Dayton, 1992).
- 23 S. W. Tsai and N. J. Pagano, "Invariant properties of composite materials," (1968).
- 24 A. Kulachenko, T. Denoyelle, S. Galland, and S. B. Lindström, *Cellulose* **19**, 793 (2012).
- 25 R. C. Neagu, E. K. Gamstedt, and F. Berthold, *Journal of composite materials* **40**, 663 (2006).
- 26 R. P. Singh, "*Thermal expansivity*" in *Mechanical and Thermophysical Properties of Polymer Liquid Crystals* (Springer, 1998).
- 27 S. Brischetto and E. Carrera, *Multidiscipline Modeling in Materials and Structures* **8**, 4 (2012).
- 28 H. Sehaqui, Q. Zhou, and L. A. Berglund, *Soft Matter* **7**, 7342 (2011).
- 29 F. Ansari, S. Galland, M. Johansson, C. J. Plummer, and L. A. Berglund, *Composites Part A Applied Science and Manufacturing* **63**, 35 (2014).
- 30 A. Boujemaoui, L. Carlsson, E. Malmström, M. Lahcini, L. Berglund, H. Sehaqui, and A. Carlmark, *ACS Applied Materials & Interfaces* **4**, 3191 (2012).
- 31 D. F. Adams and D. R. Doner, *Journal of Composite Materials* **1**, 4 (1967).
- 32 D. F. Adams and D. R. Doner, *Journal of Composite Materials* **1**, 152 (1967).
- 33 J. E. Mark, *Physical properties of polymers handbook*, Vol. 1076 (Springer, 2007).
- 34 K. Syverud, G. Chinga-Carrasco, J. Toledo, and P. G. Toledo, *Carbohydr Polym* **84**, 1033 (2011).
- 35 G. Chinga-Carrasco, Y. Yu, and O. Diserud, *Microscopy and Microanalysis* **17**, 563 (2011).
- 36 A. J. Svagan, M. A. Samir, and L. A. Berglund, *Advanced Materials* **20**, 1263 (2008).
- 37 J. Duanmu, E. K. Gamstedt, and A. Rosling, *Journal of composite materials* **46**, 3201 (2012).
- 38 G. Chinga-Carrasco and K. Syverud, *Journal of Nanoparticle Research* **12**, 841 (2010).
- 39 G. Josefsson, B. Tanem, Y. Li, P. Vullum, and E. K. Gamstedt, *Cellulose* **20**, 761 (2013).
- 40 A. Isogai, T. Saito, and H. Fukuzumi, *Nanoscale* **3**, 71 (2011).
- 41 M. Henriksson and L. A. Berglund, *Journal of Applied Polymer Science* **106**, 2817 (2007).
- 42 H. Yano and S. Nakahara, *Journal of Materials Science* **39**, 1635 (2004).
- 43 M. Henriksson, L. A. Berglund, P. Isaksson, T. Lindström, and T. Nishino, *Biomacromolecules* **9**, 1579 (2008).
- 44 H. Sehaqui, M. Allais, Q. Zhou, and L. A. Berglund, *Composites Science and Technology* **71**, 382 (2011).
- 45 Q. Cheng, S. Wang, and D. P. Harper, *Composites Part A Applied Science and Manufacturing* **40**, 583 (2009).
- 46 G. Josefsson, F. Berthold, and E. K. Gamstedt, *International Journal of Solids and Structures* **51**, 945 (2014).
- 47 K. Persson, *Doctoral Thesis Thesis*, Lund University, 2002.